



High-performance electrical discharge sawing of hard and brittle monocrystalline silicon by electroplated diamond wire

Jian Qiu^{1,2,3} · Renpeng Ge²

Received: 23 June 2021 / Accepted: 1 February 2022 / Published online: 18 February 2022
© The Author(s), under exclusive licence to Springer-Verlag London Ltd., part of Springer Nature 2022

Abstract

Nowadays, the efficiency improvement of diamond wire sawing (DWS) of photovoltaic silicon through fine wire and high-speed sawing has met the development bottleneck. This paper is a change of thinking to provide a diamond wire electrical discharge sawing (DWEDS) method to integrate the machining efficiency of DWS and electrical discharge machining (EDM), which has more advantages than the current DWS method in sawing efficiency, kerf loss, wire mark, and surface uniformity. In order to evaluate the wire sawing efficiency considering the influence of wire bow and kerf width, a new method was proposed more suitable for the efficiency evaluation of DWEDS and DWS. The efficiency of DWEDS was proved better compared with EDM and DWS. The performance of DWEDS in the aspect of silicon loss is better than that of EDM and DWS as its kerf width is smaller. The discharge effect is used to reduce the wire marks caused by the physical cutting effect of DWS. The grain sawing is better for surface roughness compared with EDM. Also, it is found that the thickness of damaged layer produced by DWEDS is related to the contribution of physical cutting and discharge effect, which is significantly lower than that of EDM. Besides, the wire consumption of DWEDS is higher than that of DWS, but the reconsolidation of the diamond wire after discharged melting will expose more grains to ensure the wire cutting capability.

Keywords Diamond wire · Grains · DWEDS · Wafer surface · Sawing efficiency · Defects · Wire bow

1 Introduction

At present, the main processing methods for silicon wafer are diamond wire sawing (DWS) and loose abrasive sawing (LAS) with slurry [1]. LAS has been rarely used in photovoltaic field, but it still has a considerable proportion of applications in semiconductor silicon wafer processing field [2]. With the development of technology, diamond wire sawing has made great progress in efficiency and quality, for example, fine wire [3], structural wire [4], and high wire speed sawing, but the reciprocating cutting problems such as wire marks and tension fluctuation still need to improve, which limit the development of surface quality and efficiency.

Generally, the way to improve the processing quality is using finer diamond wire and improving the synchronicity of moving parts to realize high-quality cutting and ensure the accuracy of the machine tool. The measures to improve the cutting efficiency are to increase wire speed and feed speed, to improve tension loss, so as to give full play to the cutting capability of diamond wire.

Wire electrical discharge machining (WEDM) has been proved to be able to cut metal and hard brittle material. Monocrystalline silicon and diamond are semi-conductor and can be used as electrodes to realize discharge machining [5]. Staufert et al. (1993) [6], Shi et al. (2008) [7], Yu et al. (2011) [8], and Yong et al. (2010) [9] studied that crystal silicon can be removed by electrical discharge machining (EDM). Yeh et al. [10] in the early crystal silicon slices applied the EDM method to manufacture silicon wafer. Hard and brittle materials with similar structure can also be cut by EDM. Rakwal and Bamberg [11] investigated the slicing of germanium crystal and analyzed the surface quality by experiment measurement. Ding et al. [12] has carried out research on multiwire cutting of semiconductor monocrystalline silicon with specific crystal orientation to improve

✉ Jian Qiu
qiu1981@163.com

¹ School of Mechanical Engineering, Qingdao University of Technology, Qingdao 266520, China

² R & D Center, Qingdao Gaoce Technology Co., LTD., Qingdao 266114, China

³ Design and Research Institute, Shenyang Machine Tool (Group) Co., Ltd., Shenyang 110142, China

the surface quality and machining accuracy. His results showed the WEDM surface with few surface cracks and low deterioration layer thickness. Rakwal and Bamberg [11] investigated the slicing of germanium wafers from single-crystal, gallium-doped ingots using wire electrical discharge machining. Material wastage during the slicing process using WEDM in combination with thin wire was analyzed to minimize sawing kerf. The thickness of the recast layer was measured by using two different chemical etchants. Liu et al. [13] and Wang et al. [14] have compared the processing efficiency of EDM and ECM for crystal silicon slice. In addition, diamond wire can be used to saw metal, such as Tönshoff et al. [15] in his research to cut pure steel.

The multiwire cutting technology of solar silicon wafers with diamond wire physical cutting combined with EDM is proposed as diamond wire electrical discharge sawing (DWEDS). This method can reduce the macro cutting force, improve the surface profile of silicon wafers and the cutting efficiency, and reduce the loss of silicon wafers, and save the production cost. Little research has been done in this field. Some scholars have conducted a small amount of scientific research. Wang et al. [16] found that low-resistance silicon may be sliced by WEDM. He combined electric discharge and anodic etching into a single process based on wire electrolytic-spark slicing strategy using hybrid oil/aqueous electrolyte. It is demonstrated that wire electrolytic-spark hybrid machining has the capability to slice and texture silicon wafers simultaneously in the photovoltaic industry. Wang et al. [17] combined the electrochemical discharge machining (ECDM) method and diamond wire sawing to saw hard and brittle insulating materials. He found the spark did not generate when the workpiece thickness is beyond 5.0 mm. It has been solved by using an oil film online coated on the diamond wire to separate it from the electrolyte. The diamond wire formed by the composition of oil and hydrogen gas can saw a thickness of 36.0 mm hard and brittle insulating workpiece. Wu and Li [18] presented a combined WEDM and fixed abrasive diamond wire saw in the field of semiconductor. It is found that this method can combine the advantages of the two machining methods on reducing the scratches of silicon surface and tool wear, and restrain the residual of carbon element compared with DWS, while improving the cutting efficiency, reducing the surface roughness and kerf width, and eliminating the recast layer and the surface heat-affected zone compared with WEDM. At present, it has been explored and studied as a cutting-edge technology in some companies in China, and launched as a prototype, and detailed demonstration was conducted for single-wire sawing, multi-wire square sawing, and slicing. The technology is suitable for photovoltaic, semiconductor silicon material cutting, and some difficult to process materials with conductor and semiconductor properties.

In this paper, the machining method of DWEDS is used for photovoltaic silicon material sawing on the basis of diamond wire cutting and EDM to integrate the machining efficiency of the two machining methods. A new efficiency evaluation method was proposed to evaluate machining efficiency of DWEDS considering the influence of wire bow and kerf dimension when compared with DWS and WEDM. Another purpose is to reduce the macro force and the wire marks caused by the physical cutting effect of DWS machining, which induce the hidden cracks and edge breakage under the cutting force. Also, surface profile caused by wire marks, material loss, and wire consumption were considered to improve the disadvantage of DWS at this stage, and to seek the technology application in production.

2 Materials and methods

Silicon is an important semiconductor material with high hardness, high brittleness, and stable chemical properties at room temperature. The processing methods for silicon materials mainly include chemical method and physical method. Chemical processing methods of silicon mainly refer to chemical etching of silicon [19], such as isotropic etching of silicon by HNO₃-HF, anisotropic etching of silicon by KOH or NaOH [20], and plasma etching. The chemical methods have not been applied in the large-scale production of silicon wafer because of its expensive equipment and great harm to operators.

Physical machining methods mainly include mechanical grinding [21, 22] and ultrasonic vibration [23]. The manufacturing technology of silicon wafers is also constantly improved. At present, the most commonly used silicon wafer manufacturing methods include cylindrical grinding, inner cylindrical grinding, band sawing [24], multiwire sawing LAS [25], and DWS [26]. The physical processing methods is the majority method.

High-purity monocrystalline silicon is an important semiconductor material. The conductivity of silicon has a great relationship with its temperature. With the increase of temperature, the conductivity increases and reaches the maximum at about 1480 °C, while when the temperature exceeds 1600 °C, it decreases with the increase of temperature. The conductivity of semiconductor crystalline silicon can be controlled from insulator to conductor.

The discharge machining of diamond wire can be realized by modifying the discharge machining device on the basis of diamond wire cutting machine, or by changing diamond wire [18] and adding the tension adjusting mechanism on the WEDM machine. The former has the advantages of constant tension, synchronous wheel system, high wire speed, and high feed speed in the cutting process; the

latter has the advantages of more comprehensive discharge parameter setting function and more sufficient discharge function.

The cutting principle of DWEDS is shown in Fig. 1a. The diamond wire is stored on the wire storage roller, passes through the guide wheel and reaches two cutting wheels, and finally returns to the wire storage roller. The silicon ingot is placed between two cutting wheels to realize cutting. The workpiece is used as the positive electrode while the wire is used as the negative tool electrode to realize electrical discharge. The sawing equipment used in the experiment is an improved DK7735 WEDM machine tool added a spring mechanism as tension adjusting function. The machine tool is shown in Fig. 1b, while the specifications of machine tool are shown in Table 1. The discharge current and gap voltage were recorded during the DWEDS machining. The surface roughness, kerf size, and surface SEM were measured, as shown in Fig. 1c.

The diameter of molybdenum wire for WEDM is 0.18 mm, while the diameter of diamond wire for DWS and DWEDS is 0.183 mm with core wire diameter 0.17 mm. The resistivity of solar grade mono-crystalline silicon used in this test is 3 Ω·cm.

The instruments used in the test is shown in Fig. 2, including Hitachi TM3030Plus scanning electron microscope for surface quality evaluation; Nikon SMZ745T stereomicroscope for dimensional accuracy measurement, such as kerf width and kerf length; Mitutoyo SJ210 surface profiler; and Nanovea 3D profiler for surface roughness measurement.

The cutting method for the comparison test includes WEDM, DWEDS, and DWS. The cutting parameters are shown in Tables 2, 3 and 4. The wire speed in the tests is constantly 660 m/min. The discharge parameters such as pulse-on time, pulse-off time, and discharge current are

Table 1 Specifications of DK7735 WEDM machine tool

Properties	Parameters
Worktable size, mm	470×710
Worktable elevation, mm	350×450
Maximum cutting thickness, mm	400
Maximum cutting efficiency, mm ² /min	> 100

the setting parameter which are set from high-frequency discharge power supply. The DWEDS machining will consume the electroplated layer of diamond wire, so that more abrasive grains will be exposed to participate in cutting. However, in order to obtain more accurate cutting data, the diamond wire was set to change after the completion of each group in the experiment and then the next group could be continued.

3 Results and discussion

3.1 Cutting efficiency and cutting area

The parameter definition of wire sawing is shown in Fig. 3. The length, width, and height of the silicon material are $L \times H \times W$. The theoretical cutting length is defined as a_p , while the kerf length l_k is the actual cutting length. The kerf width, bow, and wire bow in the cutting zone are defined as w , h , and Δh . Generally, in the field of WEDM, the cutting efficiency MRR is calculated by the cutting zone per unit time along the feed direction, as shown in Eq. (1).

$$MRR_d = L \times l_k / t \tag{1}$$

where t is the processing time, min.

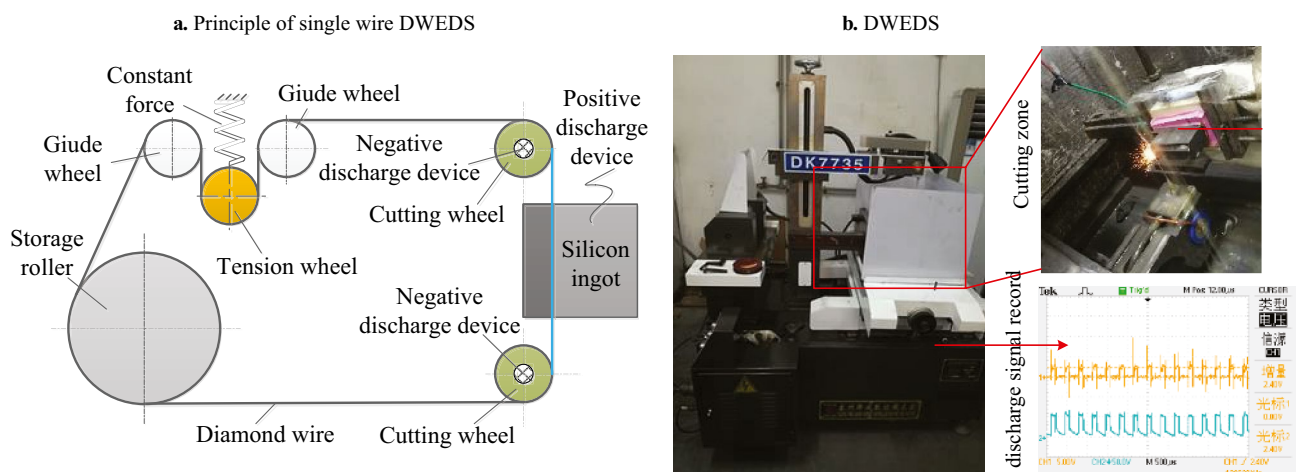


Fig. 1 Schematic of single-wire diamond wire EDM and equipment used in the sawing test. **a** Principle; **b** DWEDS tests

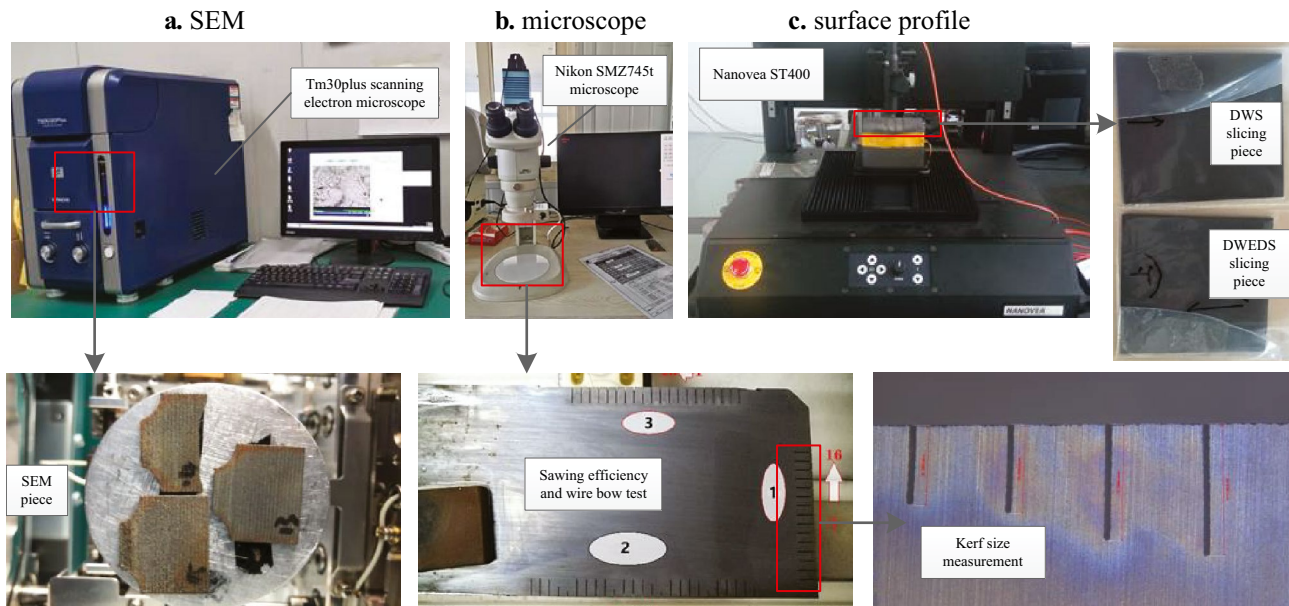


Fig. 2 Measuring instrument and measurement of test pieces. **a** SEM; **b** microscope; **c** surface profile

When the cutting widths L are the same, the material removal rate is only related to the cutting length per unit time, as expressed in Eq. (2).

$$MRR_l = H / t \tag{2}$$

However, due to the different characteristics of WEDM and DWEDS machining, the calculation method of material removal rate in Eq. (1) cannot fully reflect the cutting efficiency. WEDM is a kind of non-contact machining, the theoretical cutting length of wire is almost the same as the actual cutting length, but the removal feature of diamond wire machining is physical contact which produces wire bow, resulting in insufficient cutting, thus affecting the machining efficiency. In addition, the characteristics of kerf loss in WEDM and DWS are different, resulting in different kerf width for the same wire diameter. The DWEDS machining is

based on two machining modes of physical removal of DWS and discharge removal of WEDM; as a result, wire bow and differences on kerf dimension also exist. Therefore, a cutting efficiency evaluation method based on the material removal volume per unit time along the feed direction is proposed as shown in Eq. (3). When the material width W is the same, the area of material removal in the plane perpendicular to the wire moving direction can also be used for evaluation, as shown in Eq. (4).

$$MRR_v = V / t = w \times L \times l_k / t \tag{3}$$

$$MRR_A = V / (L \times t) = w \times l_k / t \tag{4}$$

where A is the material removal area per unit time in the plane perpendicular to the wire moving direction, $\mu\text{m}^2/\text{min}$; V is the material removal volume, mm^3 ; L is the cutting

Table 2 Comparison test parameters of WEDM and DWEDS on the kerf size, and material loss regarding electrical parameters and feed speed

Test no	Processing method	Pulse-on time (P_w), μs	Discharge current (C), A	Pulse-off time (P_p), $\times P_w \mu\text{s}$	Feed speed (v_f), $\mu\text{m/s}$	Kerf length (a_p), mm
Test 1: nos. 1–16	WEDM/DWEDS	60	3.2	5	4, 6, 8, 10	6
	WEDM/DWEDS	60	6.4	5	4, 6, 8, 10	6
	WEDM/DWEDS	60	9.6	5	4, 6, 8, 10	6
	WEDM/DWEDS	60	12.8	5	4, 6, 8, 10	6
Test 2: nos. 17–41	WEDM/DWEDS	30	6.4	3, 4, 5, 6, 7	8	6
	WEDM/DWEDS	45	6.4	3, 4, 5, 6, 7	8	6
	WEDM/DWEDS	60	6.4	3, 4, 5, 6, 7	8	6
	WEDM/DWEDS	75	6.4	3, 4, 5, 6, 7	8	6
	WEDM/DWEDS	90	6.4	3, 4, 5, 6, 7	8	6

Table 3 Efficiency and surface quality comparison test parameters

No	Processing method	Pulse-on time (P_w), μs	Discharge current (C), A	Pulse-off time (P_p), $\times P_w \mu\text{s}$	Feed speed (v_f), $\mu\text{m/s}$
Test 3: nos. 42–49	WEDM	90	4.8	2	12, 14, 16
	DWEDS	90	4.8	2	12, 14, 16, 18, 20
Test 4: nos. 50–59	WEDM	90	4.8	4	12, 14, 16, 18, 20
	DWEDS	90	4.8	4	12, 14, 16, 18, 20
Test 5: nos. 60–69	WEDM	90	4.8	6	12, 14, 16, 18, 20
	DWEDS	90	4.8	6	12, 14, 16, 18, 20
Test 6: nos. 70–84	WEDM	90	4.8	8	12, 14, 16, 18, 20, 24
	DWEDS	90	4.8	8	12, 14, 16, 18, 20, 24, 30, 36, 42
Test 7: nos. 85–100	DWS	–	–	–	4, 6, 8, 10, 12, 14, 16, 18, 20, 24, 27, 30, 32, 36, 40, 42
Test 8: no. 101–102	DWEDS	100	4.8	8	16
	DWS	–	–	–	16

length, mm; w is the kerf width, μm ; a_p is the sawing depth of kerf, mm.

Figure 4 shows the comparison of material removal rate using the traditional WEDM method and the new method considering wire bow and kerf dimension in the WEDM, DWEDS, and DWS processing, respectively. The test parameters are shown in Table 3. It can be seen that there are some differences between the two methods in the efficiency evaluation of WEDM. As the length L of silicon material in the experiment is constant, the difference shows that the kerf width of WEDM fluctuates greatly at a lower feed speed, while the kerf width is stable when the feed speed increases and matches the discharge process, as shown in Fig. 4a. There is a significant difference between the two methods in the efficiency evaluation of DWEDS and DWS, as shown in Fig. 4b, c. The difference increases with the increase of feed speed, which indicates that WEDM is more likely to cause kerf width inconsistency, and this trend deteriorates with the increase of feed speed. Therefore, the method in Eq. (3) or in Eq. (4) can better reflect the variation of kerf width. In addition, it can be seen from the figure that the material removal rate of DWEDS is higher than that of WEDM and DWS.

The efficiency comparison of the three sawing methods based on Eq. (4) proposed in this paper is shown in Fig. 5a.

It can be seen that the sawing efficiency of DWEDS is always higher than that of DWS when the pulse-on time is 90 μs , the pulse-off time is three times of pulse-on time, and the discharge current is 12.8 A. When the feed rate is lower than 20 $\mu\text{m/s}$, the efficiency of WEDM is higher than that of DWS. However, with the increase of feed rate, the discharge cutting capability cannot match the increase of feed rate, and the sawing efficiency of WEDM decreases greatly. From Fig. 5b, the sawing kerf of DWEDS machining is closer to the set kerf length 6 mm. When the feed speed is less than 20 $\mu\text{m/s}$, the kerf lengths obtained by WEDM method and DWS method appear inflection point.

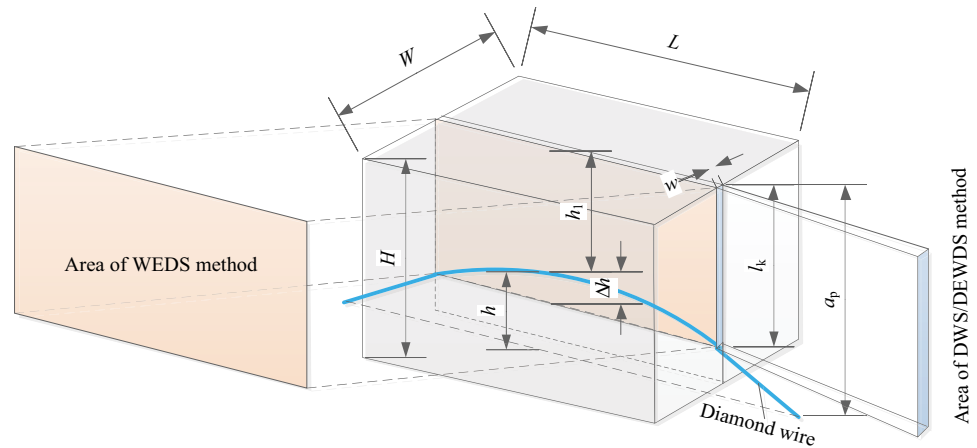
3.2 Wire bow and kerf length

When the silicon is cut at a certain sawing depth, such as 6 mm, without cutting through the silicon, the change trend of the wire bow ($h - h_1$) can be approximately equal to the sawing depth ($h_1 + \Delta h$). As shown in Fig. 3, the actual wire bow is ($h - h_1$), the actual sawing depth ($h_1 + \Delta h$) is measured, so that the wire bow [$h - (h_1 + \Delta h)$] can be obtained approximately, and the error with the actual wire bow is Δh . In Fig. 3, it can be seen that the proportion is very small, and the approximate can be ignored.

Table 4 Test of kerf width comparison of WEDM, DWS, and DWEDS with high feed speed, test parameters of thickness of damaged layer

No	Processing method	Pulse-on time (P_w), μs	Discharge current (C), A	Pulse-off time (P_p), $\times P_w \mu\text{s}$	Feed speed (v_f), $\mu\text{m/s}$	Comments
Test 9: nos. 103–128	WEDM	90	4.8	8	12, 14, 16, 18, 20	–
	DWEDS	90	4.8	8	12, 14, 16, 18, 20, 24	Damaged layer size test
	DWS	–	–	–	30, 36, 42	–
					12, 14, 16, 18, 20, 24, 27, 30, 32, 36, 40, 42	–

Fig. 3 Parameter definition of WEDM, DWS, and DWEDS



From the sawing depth distribution of the three processing methods in Fig. 5, the wire bow is large. When the discharge current is low, the wire bow of DWEDS is bigger than that of DWS. When the feed speed is low, the wire bow is very small due to non-contact removal in WEDM. When the feed speed increases beyond the discharge removal capacity, the wire bow of WEDM increases significantly. Under the condition of high discharge current, the wire bow of DWEDS is smaller than the other two machining methods, especially at high feed speed.

The kerf length can be used to indirectly evaluate the wire bow and attached cutting phenomenon which is due to that the actual wire position cannot reach the setting position, resulting in insufficient cutting, and can also be used to evaluate the cutting accuracy along the wire feed direction from the following equation.

$$l_k = h_1 + \Delta h. \quad (5)$$

In Test 2: nos. 1–25 in Table 2, the larger the pulse-on time is, the larger the kerf length is, indicating that the wire bow is smaller and the discharge removal capability is high, resulting in a high composite removal capability as the diamond wire has constant removal capability, as

shown in Fig. 6. The larger the pulse-off time, the smaller the kerf length. When the pulse-off time is larger as 5 times of pulse-on time in Fig. 6, the kerf length decreases sharply, which may be due to the weak discharge effect. The material removal is mainly an abrasive removal, but without the discharge removal function, the composite material removal capability and cutting efficiency are reduced.

According to the 1–25 cutting test data in Test 2 in Table 2, the corresponding cutting parameters show that the kerf length is stable between 5.6 and 5.9 mm when the discharge removal capability can match the feed speed, as the dotted line shown in Fig. 7. This means the electrical discharge is sufficient for the discharge effect of diamond wire sawing. When the pulse-off time increases, such as $7 \times 45 \mu\text{s}$ corresponding to $45 \mu\text{s}$ pulse-on time, and $6 \times 90 \mu\text{s}$ and $7 \times 90 \mu\text{s}$ corresponding to $90 \mu\text{s}$ pulse-on time, the discharge is insufficient, and the kerf length changes greatly. The material removal rate will not keep up with the feed speed, resulting in a larger wire bow, as the solid line shown in Fig. 7. In both cases, there is a certain linear correlation between kerf length and kerf width.

Wafer production with multi-wire sawing leads to high consumption of silicon material because of the kerf loss [27]. Using the parameters in Table 4 to test the silicon

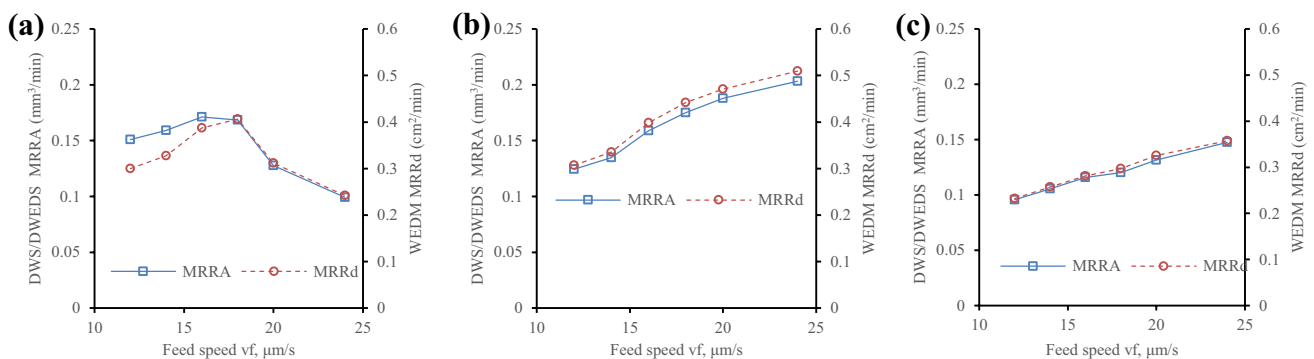


Fig. 4 Evaluation comparison of material removal rate between two methods in the WEDM, DWEDS, DWS processing. **a** WEDM; **b** DWEDS; **c** DWS

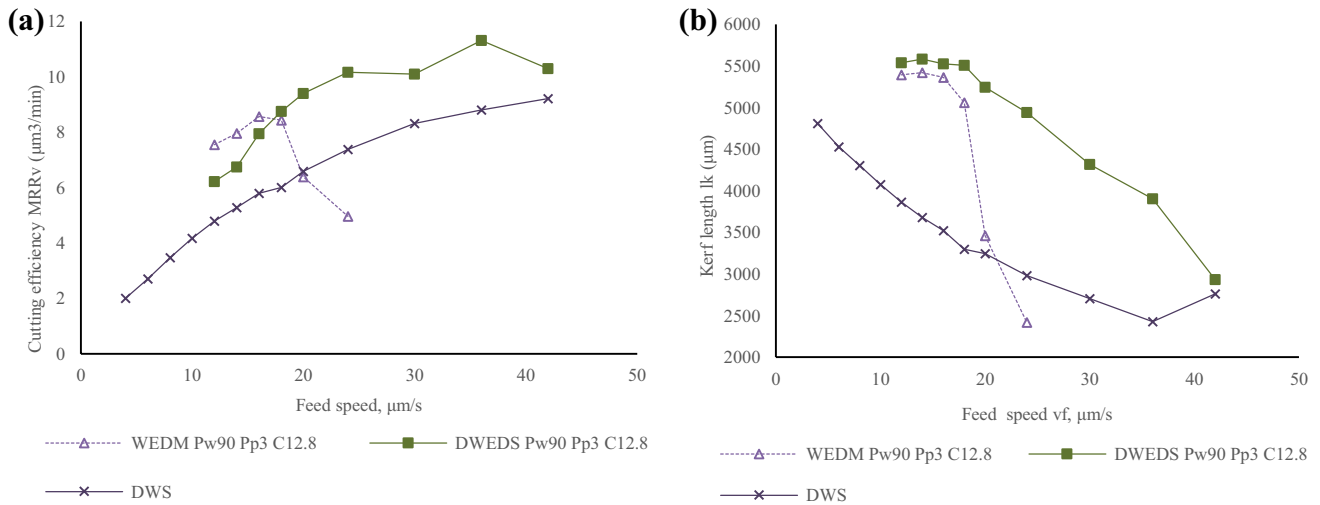


Fig. 5 Cutting efficiency and sawing depth with feed speed. **a** Cutting area per minute vs. feed speed; **b** kerf length vs. feed speed. Note: P_w90 in the figure represents pulse-on-time = 90 μs; P_p3 represents pulse-off time = 3 × pulse-on time; C12.8 represents discharge current = 12.8 A

material loss, the results are shown in Fig. 8. The kerf width of DWEDS processing is the smallest, followed by DWS and WEDM. The kerf widths of DWEDS and DWS vary little with the increase of feed speed, which shows that the consistency is fine, while the kerf width of WEDM decreases with the increase of feed speed, indicating that the discharge effect decreases with the increase of feed speed, which also proves that the material removal mode of DWEDS changes from discharge removal to physical cutting of diamond wire.

It can be found from the test on the kerf size and material loss after wire sawing in Test 1 and Test 2 in Table 2 that kerf width is related to electrical discharge parameters and feed speed. With the increase of feed speed, the kerf width decreases, as shown in Fig. 9a. The kerf width increases with the increase of discharge current. It shows that the removal capability of EDM increases with the discharge current increases, which is unfavorable to the control of kerf loss. The increase of feed speed weakens the discharge energy per

unit time, so as to reduce the kerf loss. This also shows that the silicon loss of EDM is greater than that of DWS.

Seen from Fig. 9b, the larger the discharge pulse-on time is, the larger the kerf width is, and the greater the material loss is. The larger the pulse-on time is, the smaller the kerf width is, and the trend is more linear, which indicates that the material removal loss on the kerf is proportional to the discharge pulse-on time.

With the increase of feed speed, the actual kerf length decreases, as shown in Fig. 9c, which indicates that the increase of feed rate will increase wire bow. Meanwhile, the kerf length is relatively large when the discharge current is large. In addition, for the discharge current 3.2 A, the cutting capability cannot match the feed speed when the feed speed reaches 10 mm/s, resulting in insufficient cutting.

3.3 Surface quality

The surface obtained by WEDM and DWS are shown in Fig. 10. The WEDM surface is more uniform and has no obvious wire marks, as shown in Fig. 10a. The wire marks

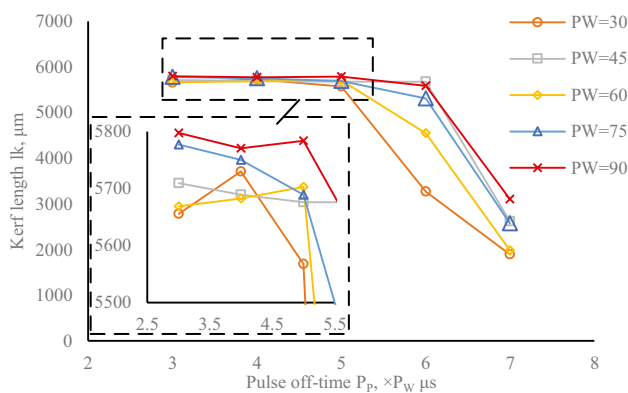


Fig. 6 Kerf length changed with pulse-off time and pulse-on time

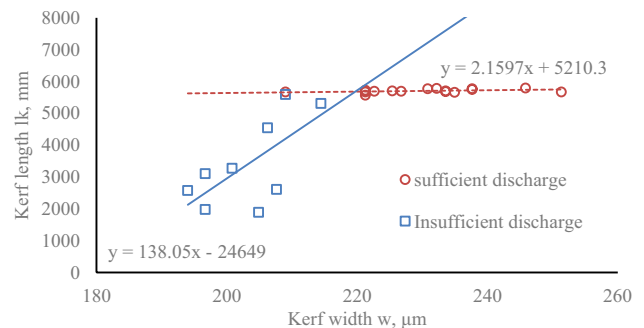
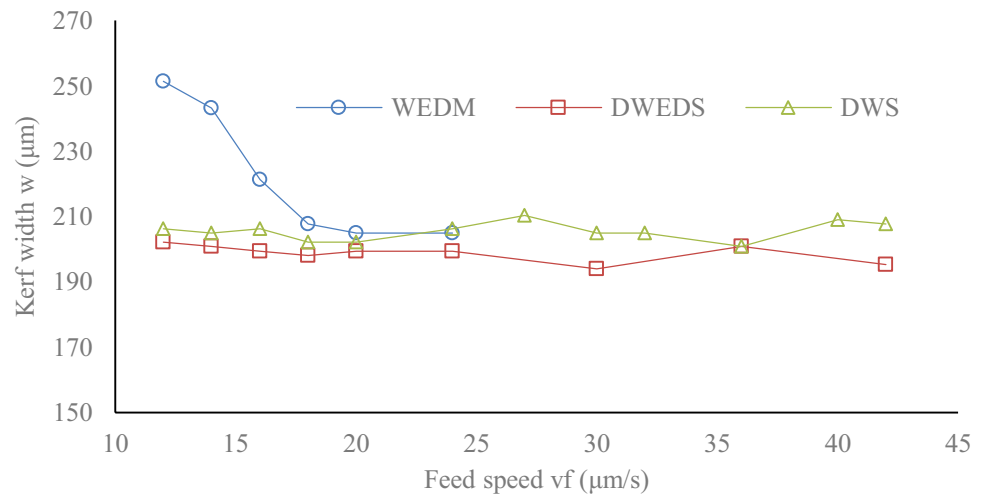


Fig. 7 Relationship between kerf length and kerf width

Fig. 8 Kerf width comparison of WEDM, DWS, and DWEDS



on the surface of DWS are obvious, showing periodic peak-valley alternation, as shown in Fig. 10b. The wire marks are caused by the lateral displacement of diamond wire during the acceleration and deceleration in the process of reciprocating sawing.

Table 5 shows the comparison of surface among WEDM, DWS, and DWEDS with parameters of pulse-on time 90 μs , discharge current 12.8 A, pulse-off time 270 μs , wire speed 11 m/s, feed speed 20 $\mu\text{m/s}$ for WEDM and DWEDS, and wire speed 11 m/s and feed speed 20 $\mu\text{m/s}$ for DWS. From the microscopic images, it can be seen that in the small area of 1.5 mm \times 1.2 mm, the surface quality of DWS is the best, followed by DWEDS. A lot of evenly distributed pits are on the WEDM surface, while the scratch marks were by micro abrasive grains on the surface processed by DWS. Different from the obvious wire marks on the macro surface of DWS, surface of DWEDS combines with the features of WEDM and DWS. In summary, from the microscopic point of view, the surface quality of DWS is the best and that of WEDM is the worst. By the action of EDM, wire marks produced by diamond wire cutting are weakened. The surface quality of DWEDS is between that of DWS and WEDM.

The actual sawing depth cannot reach the preset sawing depth 6 mm due to the wire bow generated by the force, and

even the sawing depth is only 3~4 mm in some parameter conditions. The roughness measurement length is 3 mm, among which the surface roughness obtained by DWS is the best, followed by DWEDS, and the surface roughness obtained by WEDM is the worst, as shown in Fig. 11a. The test parameters are shown in Tables 3 and 4.

From the deviation distribution of machined surface as shown in Fig. 11b, the deviation distribution of WEDM is better than that of DWEDS, and the deviation distribution of surface obtained by these two methods has more negative skew, indicating that surface consistency is better than that of DWS.

From the kurtosis coefficient in Fig. 11c, the surface obtained by DWS and DWEDS is sharper than that obtained by WEDM, in which the surface sharpness of DWS is higher at the lower feed speed 6 $\mu\text{m/s}$ and the higher feed speed 32–42 $\mu\text{m/s}$, and that of DWEDS is sharper at the feed speed 18–24 $\mu\text{m/s}$. On the whole, DWEDS method can change the surface sharpness of diamond wire cutting.

The waviness can be reflected on the surface of large size measurement of silicon wafer, as shown in Fig. 12. It can be seen that when the roughness and waviness are separated, the waviness of DWS surface is significantly higher than that of DWEDS. From the roughness analysis

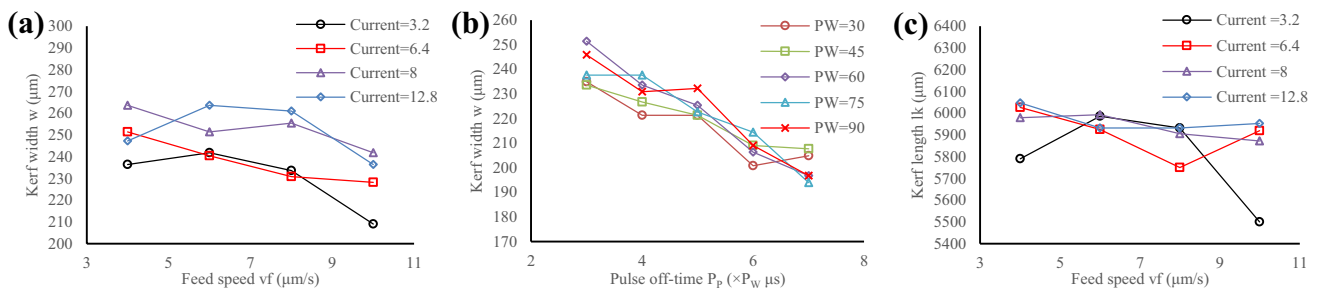


Fig. 9 Kerf width and kerf length. **a** Kerf width changed with feed speed and discharge current; **b** kerf width changed with pulse-off time and pulse-on time; **c** kerf length changed with feed speed and discharge current. Note: Current in the figures means discharge current in short

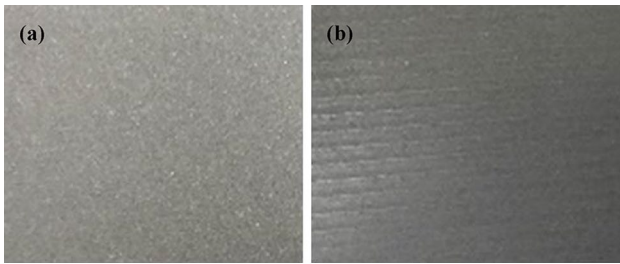


Fig. 10 Macroscopic surface contrast of WEDM and DWS, magnification 1×. **a** WEDM; **b** DWS

above, the surface roughness of DWS is lower than that of DWEDS. It also explains why the machined surface is brighter, but the wire marks are more obvious.

The surface profiles of wafer are as shown in Fig. 13. The parameters are as follows: wire speed 11 m/s, pulse-on time 100 μs, pulse-off time 300 μs, discharge current 12.8 A, feed speed 16 μm/s. For the same parameters, DWS and DWEDS methods are used to cut three repeated samples, respectively.

The left and right surfaces of the kerf are measured, with the measurement length 6.4 mm. The roughness is shown in Table 6. It can be found that whether the surfaces were on the left side or the right side of the kerf, the average roughness R_a or the highest roughness R_z , and the profile skewness coefficient R_{sk} and kurtosis coefficient R_{ku} obtained by the DWEDS method are significantly better than those obtained by the DWS method.

In the macro scale, WEDM is good for improving the wire marks, while in the micro scale, the grinding effect of diamond wire is good for improving the surface roughness. Compared with diamond wire cutting, the composite method improves the wire mark; compared with WEDM, the surface roughness is improved. The purpose of DWEDS machining is to give full play to the advantages of high surface quality by DWS and the advantages of distribution consistency of surface profile by WEDM.

The measurement points on wafer surface for the comparison with different electrical parameters are shown in Fig. 14. Eight points along the feeding direction on the left and right lines of the upper half of the wafer were measured. The surface roughness indices obtained by comparing

Table 5 Comparison of surface SEM obtained by WEDM, DWS, and DWEDS

Magnification	WEDM	DWS	DWEDS
X100			
X400			
X1000			

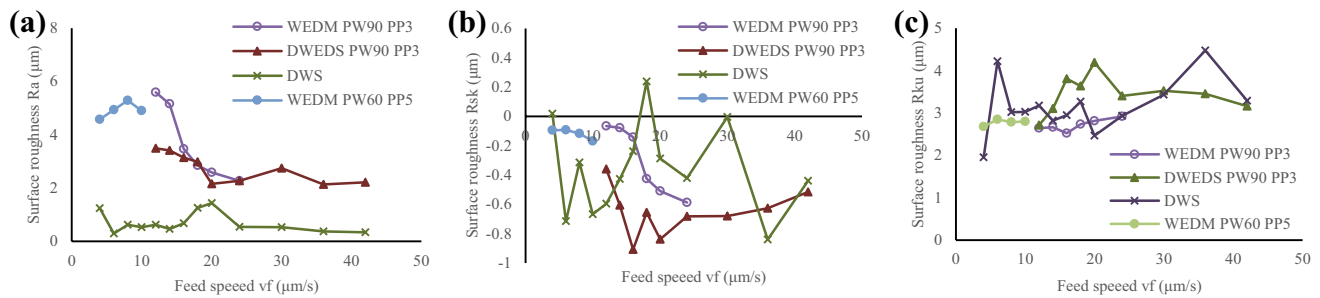


Fig. 11 Comparison of average roughness of WEDM, DWS, and DWEDS. **a** Average roughness; **b** skewness coefficient; **c** kurtosis coefficient

different electrical parameters are shown in Fig. 15. The test parameters are shown in Table 3. The surface roughness R_a by higher power machining is worse than that of lower power when the pulse-on time, pulse-off time, and feed speed are the same. The surface with lower power has more negative deflection than the surface with higher power, which indicates that the machined surface is better. The kurtosis coefficient of the surface with higher power is closer to 3 than that of lower power, indicating that the height distribution is closer to the normal distribution.

In Fig. 15b, the parameters with different pulse-on time and other parameters are the same; the average surface roughness R_a of 120 μs pulse-on time is larger than that of 90 μs pulse-on time, which indicates that the larger discharge pulse-on time will increase the proportion of material removal by EDM when the material removal rate matches feed rate. This will result in the increase of surface roughness. The same results can be obtained from R_{sk} curve. Most of R_{sk} values are better reflected in the small discharge pulse-on time. As shown in Fig. 15a, the kurtosis coefficient R_{ku} with smaller roughness is usually larger, which indicates that surface with more discharge erosion removal is poorer in roughness distribution, but the surface texture distribution is more uniform and consistent. This conclusion is the same as that reflected by macroscopic images.

From the curve of average roughness and skewness coefficient of roughness in Fig. 15c, it can be seen that the surface

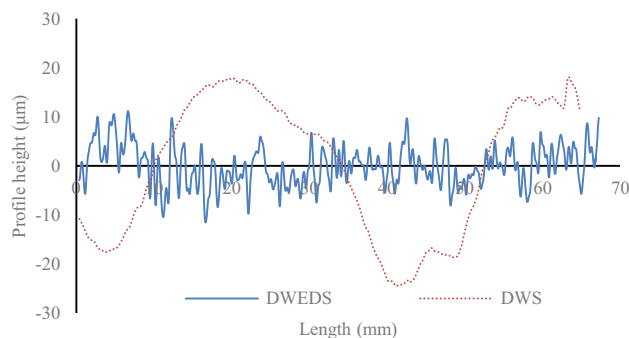


Fig. 12 Waviness curve of DWS and DWEDS

roughness is better when feed speed is higher when other parameters are the same, which is contrary to the conclusion of DWS machining. The results show that cutting capability of wire in the DWEDS process with these parameters is enough to ensure the material removal at feed speed 30 $\mu\text{m/s}$ and 60 $\mu\text{m/s}$. At this time, the surface roughness with lower feed speed is poor due to that the electro erosion effect is more obvious than that of higher feed speed. The conclusion reflected by the kurtosis coefficient also shows that the lower the feed speed will cause the increase of the electro erosion effect, and the proportion of the discharge removal to the material will increase when discharge capacity is sufficient.

3.4 Surface defects

The influence of discharge current on the surface morphology of silicon wafer was compared. The surface morphologies with pulse-on time 75 μs , pulse-off time 525 μs , feed 6 $\mu\text{m/s}$, low discharge current 3.2 A, and high discharge current 12.8 A are shown in Fig. 16. The results show that the eclipsed pits of wafer surface in Fig. 16a, c obtained by WEDM at different discharge currents are larger than those obtained by DWEDS as shown in Fig. 16b, d with low discharge current 3.2 A and high discharge current 12.8 A, respectively. Whether it is low discharge current 3.2 A or high discharge current 12.8 A, the surface quality of DWEDS is obviously better than that of WEDM.

From the longitudinal section of silicon wafer, the thickness of the damaged layer on the machined surface [28, 29], including wire mark, electric corrosion pit, and sub-surface cracks [30, 31], can be found. The parameters in the test are shown in Table 4 with parameters of pulse-on time 90 μs , pulse-off time 270 μs , discharge current 12.8 A, and feed speed 12–24 $\mu\text{m/s}$. The curves of damaged layer thickness changing with feed speed are statistically obtained as shown in Fig. 17a. The thickness of surface damaged layer decreases with the increase of feed speed, where the thickness of surface damaged layer obtained by WEDM is the largest, followed by DWEDS, and DWS is the smallest. The thicknesses of surface damaged layer of DWEDS and DWS are closer.

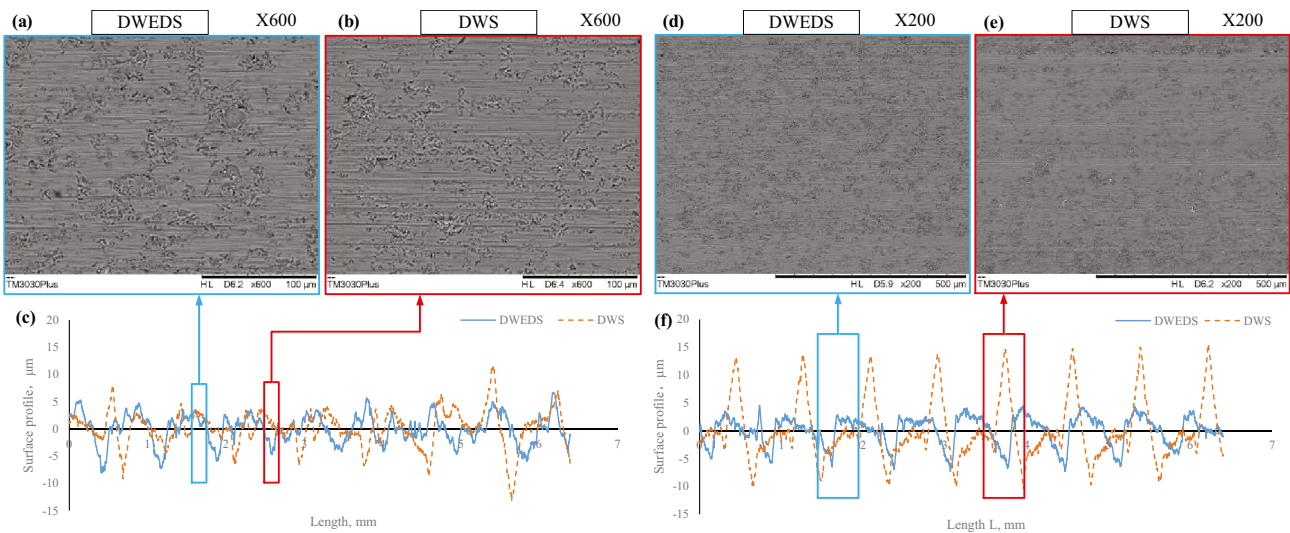


Fig. 13 Surface profile comparison of wafer. (a–c) Left side surface of kerf; (d–f) right side surface of kerf

The cumulative silicon material losses including kerf loss and damaged layer loss are shown in Fig. 17b. The cumulative silicon loss of the three machining methods decreased with the increase of feed speed, where DWS and DWEDS show little change with feed speed and have better consistency. The cumulative silicon loss of DWEDS is very close to that of DWS, and with the increase of feed speed, the cumulative loss of DWEDS has a greater advantage.

Figure 17c–e show the SEM micrograph of the damaged layer corresponding to the three processing methods with parameters of pulse-on time 90 μs, pulse-off time 270 μs, discharge current 12.8 A, and feed speed 24 μm/s. The thickness of the surface damaged layer obtained by WEDM is the largest of 76 μm, while the surface damage of DWEDS and DWS is similar, 41 μm and 34 μm, respectively.

At high energy, for the hard and brittle material, the crack will expand rapidly, and even reach the crystal region, which makes the thickness of the damaged layer increase rapidly [32]. In addition, the kerf of WEDM will affect the WEDM performance inducing gap phenomena [33].

3.5 Loss of diamond wire

The surface morphologies of diamond wire for DWEDS are shown in Fig. 18, where Fig. 18a is the surface morphology

of unused diamond wire, Fig. 18b is the surface morphology of diamond wire after cutting 13,425 mm² silicon with DWS method, and Fig. 18c is the surface morphology of diamond wire after cutting 14,895 mm² silicon with DWEDS method.

Comparing the wire surface morphologies before and after machining, it can be seen that:

1. Before machining, the abrasive is wrapped by electroplated layer on diamond wire, which prevents the cutting effect of the abrasive in the initial stage of cutting from being fully exerted, and the cutting capability of the new wire is limited, as shown in Fig. 18a.
2. After a certain amount of silicon sawing by DWS, as shown in Fig. 18b, some abrasive grains appear and wear occurs. The electroplated layer is still in good condition.
3. After the DWEDS cutting, the electroplated layer on the diamond wire surface shows cracks, and the electroplated layer accumulates around the diamond grains, which means that the electroplated layer melts and then solidifies again during the discharge process, and cracks

Table 6 Surface roughness of large size measurement of wafer

Position	Method	R_a (μm)	R_q (μm)	R_z (μm)	R_{sk}	R_{ku}
Left (a, b, c)	DWEDS	2.256	2.648	9.742	-0.380	2.186
	DWS	4.125	5.539	24.131	0.817	3.227
Right (d, e, f)	DWEDS	2.041	2.495	10.352	-0.022	2.664
	DWS	2.298	3.011	13.473	-0.409	3.168

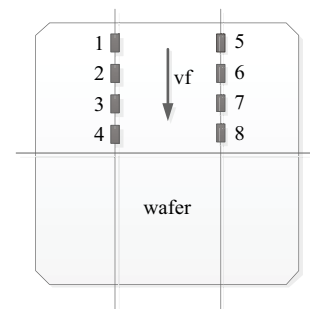


Fig. 14 Roughness measuring points on the wafer by DWEDS for the comparison with different electrical parameters

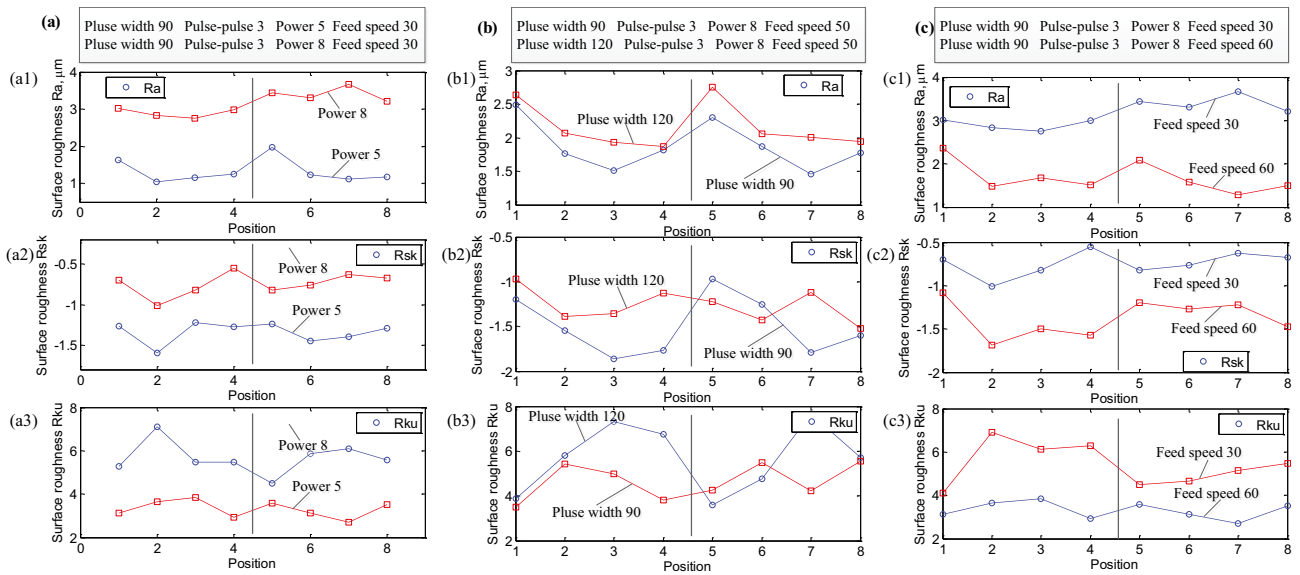


Fig. 15 Surface comparison of DWEDS with different discharge parameters

are formed under the cooling effect of cutting fluid, as shown in Fig. 18c. In the melting state, the electroplated layer makes the diamond grains exposed, thus forming a

self-sharpening effect on the worn abrasive grains, and the remelted electroplated layer strengthens the consolidation of abrasive grains. From this point of view, the

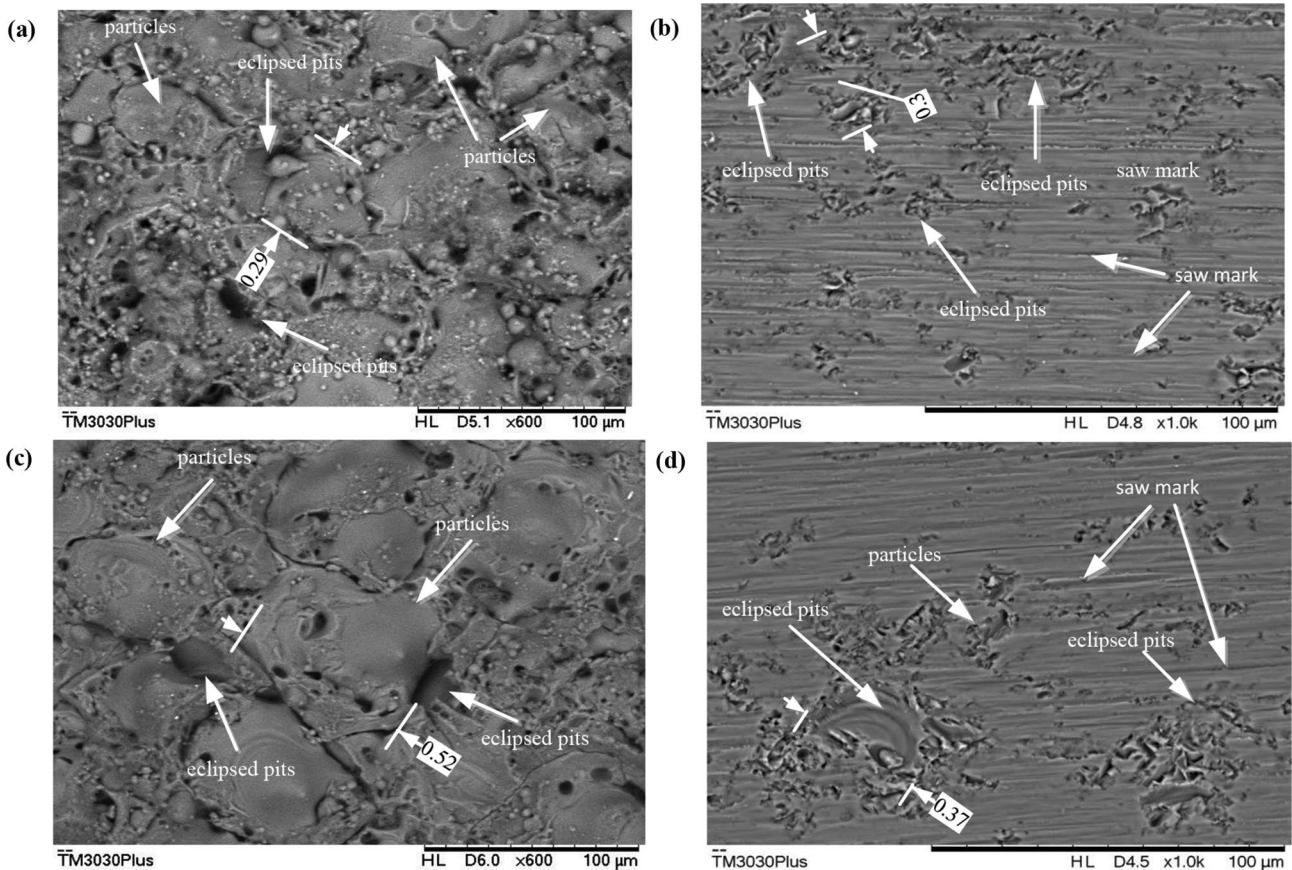


Fig. 16 Influence of discharge current on the micro defects of sawing surface. **a** Discharge current 3.2 A, WEDM; **b** discharge current 3.2 A, DWEDS; **c** discharge current 12.8 A, WEDM; **d** discharge current 12.8 A, DWEDS

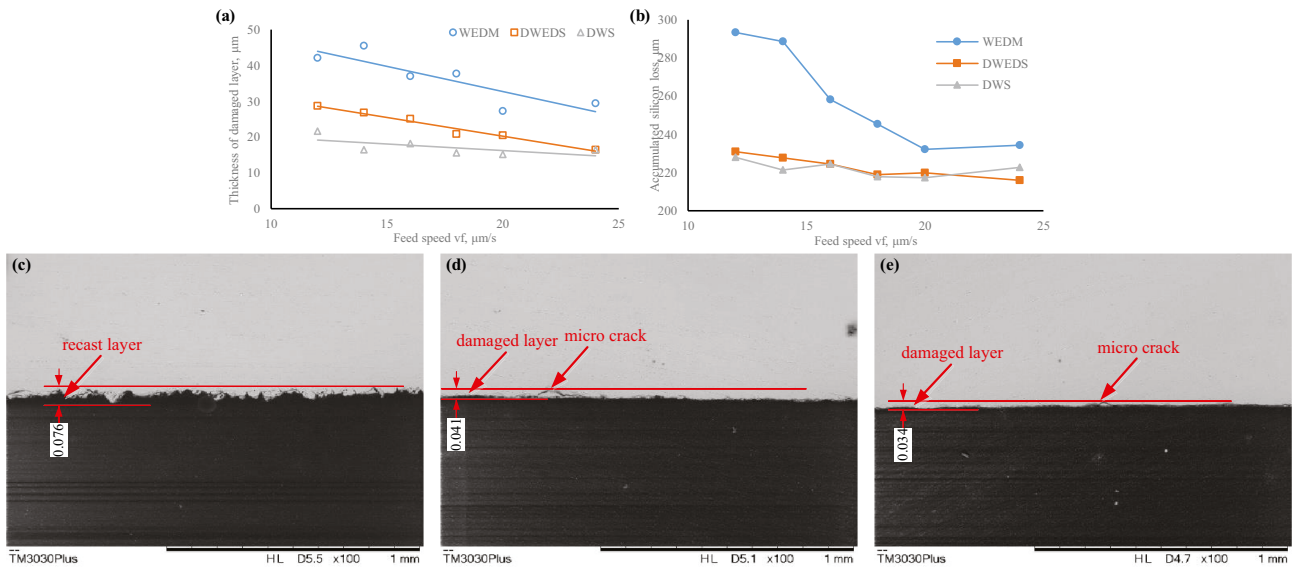


Fig. 17 Thickness of damaged layer by the three machining methods. **a** The trend of thickness of damaged layer with feed speed; **b** the trend of cumulative silicon loss with feed speed; **c** WEDM 76 μm ; **d**

DWEDS 41 μm ; **e** DWS 34 μm . Pulse-on time 90 μs , pulse-off time 270 μs , discharge current 12.8 A, feed speed 24 $\mu\text{m/s}$

abrasive self-sharpening of DWEDS has certain processing advantages, which can ensure the cutting capability of diamond wire stability and achieve high-performance sawing.

From the perspective of the loss of electrodeposited layer:

1. The diameter of the diamond wire before cutting is 142.7 μm .
2. The diameter of the diamond wire after DWS sawing is 141 μm . The diameter loss is 1.7 μm .
3. The diameter of the diamond wire after the DWEDS sawing is 139.7 μm . The diameter loss is 3 μm .

The wire diameter loss of DWEDS is higher than that of DWS. Some scholars also think that the wire diameter loss

of DWEDS processing is lower than that of diamond wire processing [18]. The conclusion difference is related to the selected discharge parameters.

3.6 Machining process of DWEDS

The actual discharge power of diamond wire with discharge peak current 12.8 A in the discharge sawing of silicon is greater than that of discharge current 8 A. As shown in Fig. 19a, the discharge power is proportional to the discharge current. The actual discharge mean current of higher discharge peak current in Fig. 19b is slightly lower than that of lower peak current, while the corresponding voltage of higher peak current is higher than that of lower discharge peak power in Fig. 19c.

When the discharge peak current is the same but the pulse-on time is different, the mean power of pulse-on time 120 μs is slightly higher than that of 80 μs , as shown in Fig. 19d. The

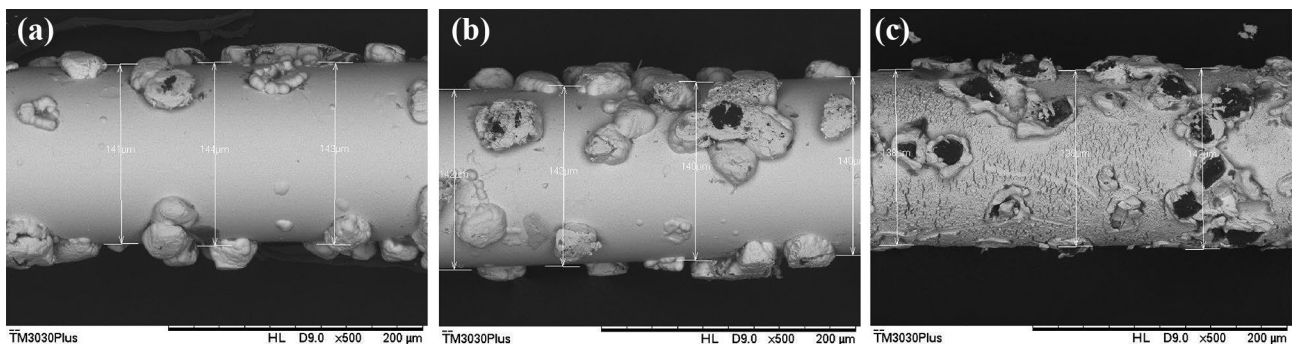


Fig. 18 Surface SEM of diamond wire of DWS and DWEDS. **a** Before processing; **b** after DWS processing; **c** after DWEDS processing

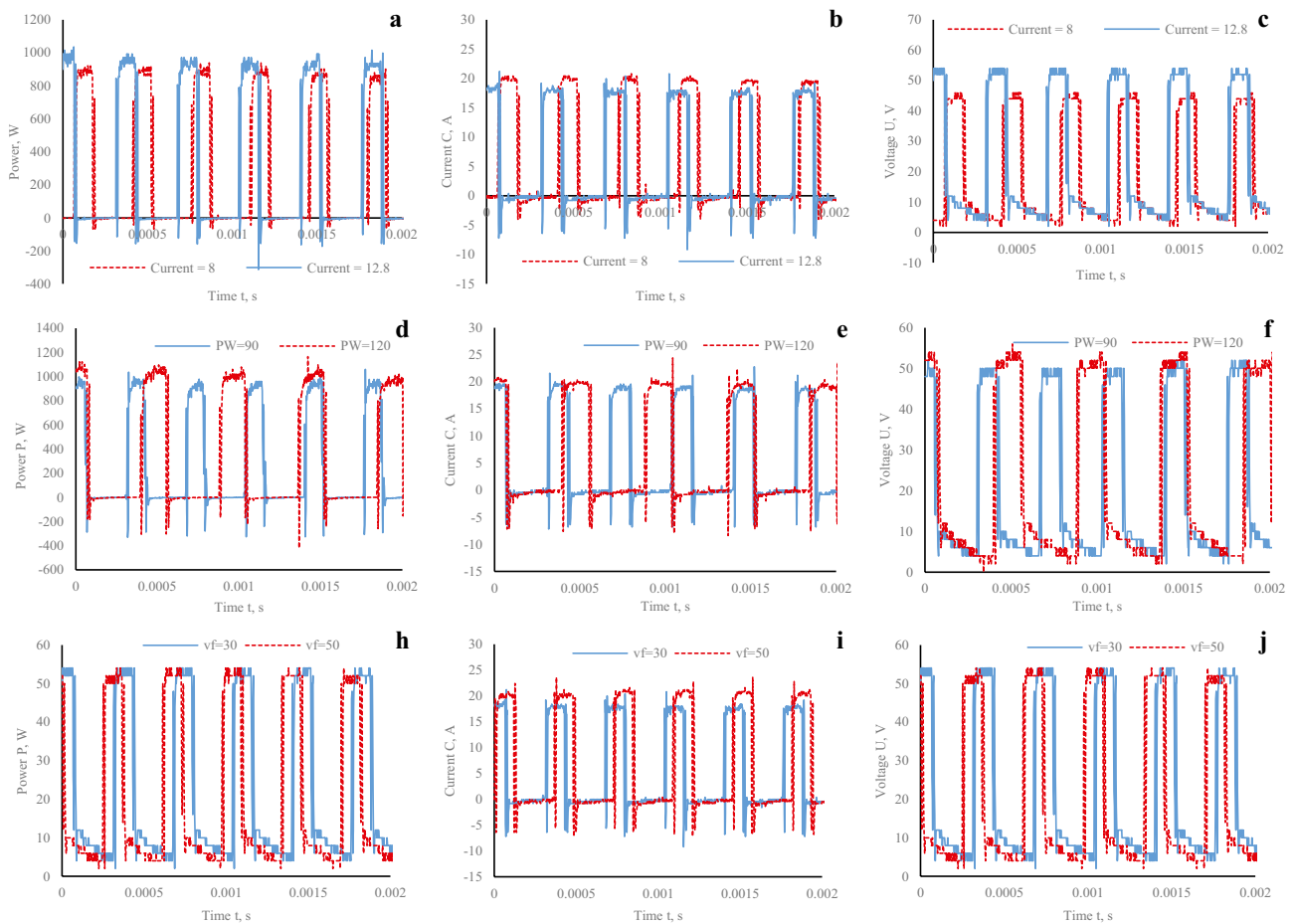


Fig. 19 Discharge power, discharge current, and voltage with different discharge peak current, **a** mean power, **b** mean current, **c** voltage (pulse-on time 90 μ s, pulse-off time 270 μ s, feed 30 μ m/s, discharge peak current 8 A and 12.8 A). Different pulse-on time, **d** power, **e** mean current, **f** voltage (pulse-on time 90 μ s and 120 μ s, pulse-off

time 270 μ s and 360 μ s, feed 30 μ m/s, discharge peak current 12.8 A). **g** Different feed speed, **h** power, **i** discharge current, **j** voltage (pulse-on time 90 μ s, pulse-off time 270 μ s, feed 30 and 60 μ m/s, discharge peak current 12.8 A)

pulse-on time has no obvious effect on the meandisc current, as shown in Fig. 19e. The distribution of voltages during sawing is the same as the conclusion of discharge power (Fig. 19f).

Without changing the discharge parameters, the power waveforms with feed rates of 30 μ m/s and 60 μ m/s are almost unchanged, as shown in Fig. 19h. However, with the increase of feed speed, the contact between diamond wire and silicon workpiece is closer. Compared with the test with low feed speed, it is easier to form a short circuit, resulting in a higher discharge mean current and a lower discharge mean voltage, as shown in Fig. 19i, j. This phenomenon will be more obvious when the cutting capability of diamond wire cannot keep up with the increase of feed speed. In this case, wire bow will increase, which will increase the contact length between diamond wire and silicon workpiece.

It can be seen from the discharge waveforms of the above tests that under these setting parameters, the discharge effect of diamond wire is obvious, which indicates that the composite cutting effect of DWEDS is significant.

4 Conclusions

In this paper, a machining method of DWEDS combined DWS with EDM is used for solar grade crystalline silicon processing. The machining performance of DWEDS was compared with that of WEDM and DWS. The following conclusions can be drawn in the research:

1. A new method for evaluating material removal rate considering wire bow and kerf dimension in the WEDM, DWEDS, and DWS processing was proposed and proved more suitable for the evaluation of DWEDS and DWS.
2. DWEDS has more advantages than WEDM in machining quality and silicon material loss, which can replace WEDM. For sawing efficiency, WEDM efficiency is slightly higher than that of DWEDS under feed speed lower than 20 μ m/s as the discharge removal of DWEDS in the condition is the main material removal mode. With the increase of feed speed, the material removal

effect of WEDM is weakened, and the physical cutting effect of diamond wire plays the main role.

3. DWEDS can replace DWS in cutting kerf, sawing efficiency, and surface consistency. But the surface quality of the two processing methods has their own characteristics as the two kinds of surface are formed with different surface formation mechanisms. The surface of DWEDS is characterized by melting pits and micro cracks while DWS is characterized by wire marks and cracks. The proportion of the pits and cracks is related to the matching of electrical parameters and physical cutting parameters. In addition, the diameter loss of diamond wire in the DWEDS is higher than that of DWS as the electric discharge makes the electroplated layer of diamond wire melt and recondense, which has the self-sharpening effect of abrasive on diamond wire and ensures continuous wire cutting capability.
4. In the DWEDS, the proportion of the discharge removal and abrasive grain removal modes is related to the feed rate and discharge parameters. The discharge removal capability is related to the discharge parameters and the contact length between diamond wire and workpiece. The physical removal capability is related to the matching of feed speed and wire speed, as well as the cutting performance of diamond wire.

Author contribution Jian Qiu: conceptualization; methodology; data curation; investigation; formal analysis; supervision; writing—original draft; visualization. Renpeng Ge: validation, investigation, equipment.

Funding This work was supported by the National Independent Innovation Demonstration Zone of Shandong Peninsula, Shandong, China.

Availability of data and material All allowed data has been provided in the manuscript.

Declarations

Ethics approval This work has no potential conflicts of interest. This work has no research involving Human Participants and/or Animals.

Consent to participate Not applicable.

Consent for publication Not applicable.

Competing interests The authors no competing interests.

References

1. Nasch PM, Park JE, Jodlowski T, Yin M (2012) Thin wafer thickness stability in multi-wire saw. In: Proceedings of the 27th EUPVSEC, pp. 1064–1067
2. Kaminski S, Wagner T, Rietzschel R, Futterer W, Funke C, Moller HJ (2010) The role of the slurry transport in multi-wire sawing of solar silicon wafers. In: Proceedings of the 24th EUPVSEC, pp. 1312–1317
3. Zhang M, Liu Z, Pan H (2021) Effect of no-load rate on recast layer cutting by ultra fine wire-EDM. *Chinese J Aeronaut* 34(4):24–131
4. Oliver A, Björn H, Kirsten S (2014) Structured wire: from single wire experiments to multi-crystalline silicon wafer mass production. *Sol Energy Mater Sol Cells* 131:58–63
5. Hsu FC, Tai TY, Vo VN (2013) The machining characteristics of polycrystalline diamond (PCD) by micro-WEDM. *Procedia CIRP* 6:262–267
6. Stauffert G, Dommann A, Lauger D (1993) Behaviour of a silicon spring fabricated by wire electro-discharge machining. *J Micro-mech Microeng* 3(4):232–235
7. Shi Y, Huang YH, Tian ZJ (2008) The development of slicing method for silicon ingot with WEDM. *Electromach Mould* 5:67–71. (in Chinese)
8. Yu PH, Lee HK, Lin YX (2011) Machining characteristics of polycrystalline silicon by wire electrical discharge machining. *Adv Manuf Proc* 26(12):1443–1450
9. Yong BI, Liu ZD, Qiu MB (2010) New cutting technology of solar-cell silicon wafers. *J Mater Sci Eng* 28(4):582–581
10. Yeh C, Wu KL, Lee JW (2013) Study on surface characteristics using phosphorous dielectric on wire electrical discharge machining of polycrystalline silicon. *Int J Adv Manuf Technol* 69(1–4):71–80
11. Rakwal D, Bamberg E (2009) Slicing, cleaning and kerf analysis of germanium wafers machined by wire electrical discharge machining. *J Mater Proc Technol* 209(8):3740–3751
12. Ding H, Liu ZD, Qiu MB (2015) Study of multi-cutting by WEDM for specific crystallographic planes of monocrystalline silicon. *Int J Adv Manuf Technol* 84(5–8):1201–1208
13. Liu ZD, Wang W, Tian ZJ, Qiu MB, Huang YH (2008) Research on high efficiency slicing of EDM and ECM on solar wafer slicing. *China Mech Eng* 14:1673–1677. (in Chinese)
14. Wang W, Liu ZX, Zhang W, Huang YH (2011) Abrasive electrochemical multi-wire slicing of solar silicon ingots into wafers. *CIRP Ann Manuf Technol* 60:255–258
15. Tönshoff HK, Denkena B, Apmann HH (2003) Diamond tools for wire sawing metal components. *Key Eng Mater* 250:33–40
16. Wang W, Liu ZD, Tian ZJ (2009) High efficiency slicing of low resistance silicon ingot by wire electrolytic-spark hybrid machining. *J Mater Proc Technol* 209(7):3149–3155
17. Wang J, Fu C, Jia Z (2017) Cutting of hard and brittle insulating materials using spark discharge-assisted diamond wire sawing. *J Mater Proc Technol* 252:225–232
18. Wu X, Li S (2018) Experimental investigations of a hybrid machining combining wire electrical discharge machining (WEDM) and fixed abrasive wire saw. *Int J Adv Manuf Technol* 95:2613–2623
19. Panek P, Lipiński M, Dutkiewicz J (2005) Texturization of multicrystalline silicon by wet chemical etching for silicon solar cells. *J Mater Sci* 40(6):1459–1463
20. Chen C, Jiang L, Zhang P (2018) Simple method to measure the etching rate of monocrystalline silicon in KOH solution. *Micro Nano Lett* 13(4):481–485
21. Gao S, Kang R, Dong Z (2013) Edge chipping of silicon wafers in diamond grinding. *Int J Mach Tools Manuf* 64:31–37
22. Wang ZG, Kang RK, Zhou P (2019) Ultra-precision grinding of monocrystalline silicon reflector. *Guangxue Jingmi Gongcheng/Opt Precis Eng* 27(5):1087–1095
23. Liang Z, Wu Y, Wang X (2010) A new two-dimensional ultrasonic assisted grinding (2D-UAG) method and its fundamental performance in monocrystal silicon machining. *Int J Mach Tools Manuf* 50(8):728–736

24. Yin CQ, Zhou L (2010) Characterization of band sawing dusts generated in cutting of multi-crystalline silicon ingots. *J Wuhan Univ Technol (Mater Sci Ed)* 25(06):56–59
25. Wu H, Yang C, Melkote SN (2014) Effect of reciprocating wire slurry sawing on surface quality and mechanical strength of as-cut solar silicon wafers. *Precis Eng* 38(1):121–126
26. Kumar A, Melkote SN (2018) Diamond wire sawing of solar silicon wafers: a sustainable manufacturing alternative to loose abrasive slurry sawing. *Procedia Manuf* 21:549–566
27. Schwinde S, Berg M, Kunert M (2015) New potential for reduction of kerf loss and wire consumption in multi-wire sawing. *Sol Energy Mater Sol Cells* 136:44–47
28. Ge MX, Liu ZD, Shen LD (2016) Thickness measurement of deterioration layer of monocrystalline silicon by specific crystallographic plane cutting of wire electrical discharge machining. *J Mater Sci Mater Electr* 27(9):9107–9114
29. Mouralova K, Prokes T, Benes L, Bednar J (2019) The influence of WEDM parameters setup on the occurrence of defects when machining hardox 400 steel. *Materials* 12:3758
30. Gao L, Liu ZD, Qiu MB (2011) Damaged layer of monocrystalline silicon cut by wire electrical discharge machining. *J Chin Ceram Soc* 39(5):874–879(6)
31. Ge MX, Liu ZD, Chen HR (2017) Machining damage of monocrystalline silicon by specific crystallographic plane cutting of wire electrical discharge machining. *J Mater Sci Mater Electr* 28(12):8437–8445
32. Gao L, Liu ZD, Qiu MB (2011) Analysis on deterioration layer and cracks of monocrystalline silicon cut by WEDM. *China Mech Eng* 9:86–91
33. Kitamura T, Kunieda M (2014) Clarification of EDM gap phenomena using transparent electrodes. *CIRP Ann Manuf Technol* 63(1):213–216

Publisher's Note Springer Nature remains neutral with regard to jurisdictional claims in published maps and institutional affiliations.